

Auxiliary Maximum Likelihood Estimation for Noisy Point Cloud Registration



DUKE UNIVERSITY/COMPUTER SCIENCE

Cole Campton

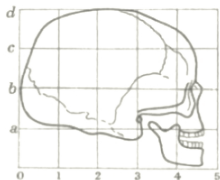
Xiaobai Sun

September 26 2019

Outline

1. Problem Introduction
2. Related Works
3. Contributions
4. Experimental Results
5. Conclusion

Shape Matching in Point-set Registration



Human skull



Chimpanzee skull



Baboon skull

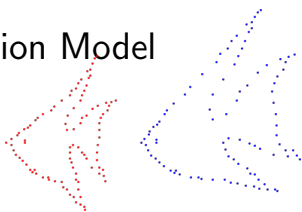
- ◇ **Registration** of point sets is an important data analytic task
- ◇ **Shapes** contain semantic meanings of topology and geometry
- ◇ **Deformation** Nonrigid, nonlinear mapping

[Thompson, 1992]

Applications

- ▶ 3-D scanners: data points from multiple views are fused together via registration to overcome acquisition limitations [[Lempitsky and Boykov, 2007](#)].
- ▶ Radiation therapy guided by medical imaging: accurate registration is critical to precise target localization and accurate dose estimation [[Simon et al., 2015](#)].
- ▶ Label propagation: semi-automatic segmentation [[Heckemann et al., 2006](#)].

Generic Registration Model



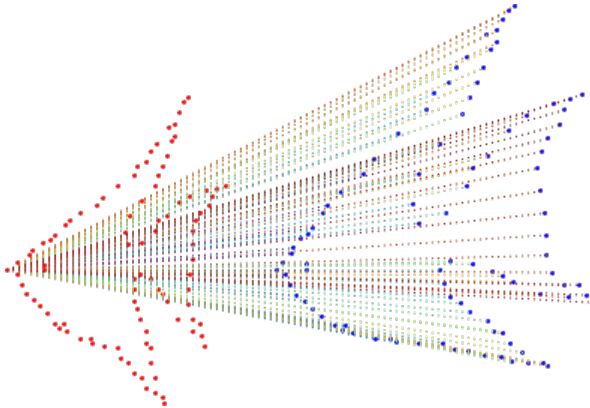
Domain point set A Codomain point set B .

$$\inf_{f \in F} D(f, A, B)$$

- ▶ F : model family, feasibility/regularization conditions
- ▶ D : measure of model-data fitting

We will specify our conditions for F and choice of D

Uncertainty in Point Correspondance



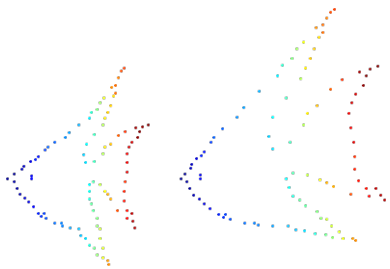
A single point in A may have multiple matching candidates in B

Global View in Matrix form

$$\Delta(f) = \begin{pmatrix} \delta_{1,1} & \delta_{1,2} & \cdots & \delta_{1,n} \\ \delta_{2,1} & \delta_{2,2} & \cdots & \delta_{2,3} \\ \vdots & \vdots & \ddots & \vdots \\ \delta_{n,1} & \delta_{n,1} & \cdots & \delta_{n,n} \end{pmatrix}, \quad \begin{aligned} \delta_{i,j} &= \delta(b_i = f(a_j)) \\ \delta_{ij} &\in [0, 1] \end{aligned}$$

- ▶ Δ is a **permutation** matrix with ideal, combinatorial setting
- ▶ Δ is **doubly stochastic** in the present work in order to account for uncertainty

Ideal Case

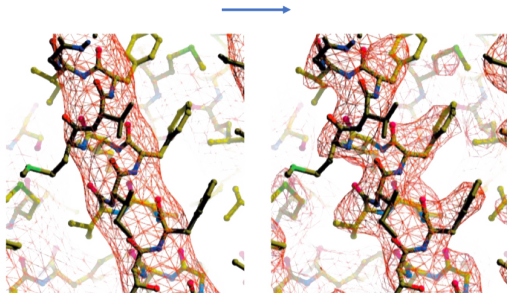
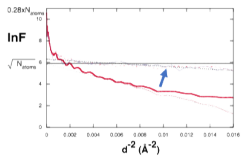


Ideal point-set registration:
corresponding points in same color

$$\Delta = \begin{pmatrix} 1 & 0 & \cdots & 0 \\ 0 & 1 & \cdots & 0 \\ \vdots & \vdots & \ddots & \vdots \\ 0 & 0 & \cdots & 1 \end{pmatrix}$$

Ideal mapping among $O(n!)$
permutations

Spectral Noise in Cryo-Electron Microscopy



[Terwilliger et al., 2018]

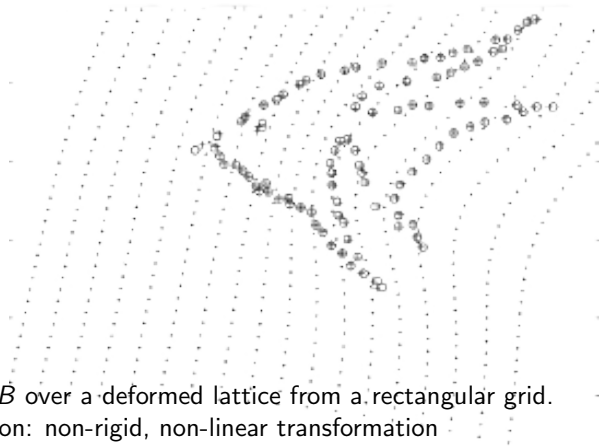
Stochastic Mappings

In the presence of Gaussian noise in point sets, Δ becomes doubly stochastic

$$\Delta = \begin{pmatrix} .7 & .2 & .1 & \dots & 0 \\ .2 & .8 & 0 & \dots & 0 \\ .1 & .0 & .8 & \ddots & \vdots \\ \vdots & \vdots & \ddots & .8 & .1 \\ 0 & 0 & \dots & .1 & .8 \end{pmatrix}$$

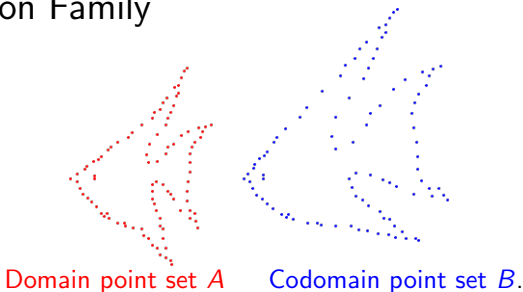
- $\text{nnz}(\Delta)$ is up to n^2 , instead of n
- the space of doubly stochastic mappings is BIG
- + the feasible mappings are limited by shapes & deformation types

Deformation



Point set B over a deformed lattice from a rectangular grid.
Deformation: non-rigid, non-linear transformation

Deformation Family



Desirable properties (regularization conditions)

- ▶ symmetric registration: $B = f(A)$ $A = f^{-1}(B)$
- ▶ neighborhood preserving
- ▶ not sensitive to noise in data

Data Fitting Measure: GH Distance

Among the Gromov-Wasserstein distance family,¹ we focus on L_2 -Gromov-Hausdorff (GH_2) distance

$$d_{\text{GH}_2}(A, B) = \inf_f \|d_A(a, a') - d_B(f(a), f(a'))\|_2$$

where f is isometric

- ▶ $\|d_A(a, a') - d_B(f(a), f(a'))\|_2$ is a functional in f
- ▶ “ $d_{\text{GH}}(A, B) = 0$ ” \implies “ (A, d_A) and (B, d_B) are isometric”
- ▶ $d_{\text{GH}}(A, B)$ is **invariant** to isometric mappings between A and B ;
a critical extension, distinction from Hausdorff set distance

¹[Mémoli, 2011]

GH Distance: Applications & Advances

- ▶ Used for shape matching ²
- ▶ Connections to Heat Kernel Signature, intrinsic, foundation to multiscale methods. ³ ²
- ▶ Lower bounds present approximations by constrained linear programs ²
- ▶ Choices of point distances d_A , d_B and their related intrinsic similarity are well understood ²

²[Mémoli, 2011]

³[Sun et al., 2009]

Limitations/Gaps in Related Existing Work

- Computational complexity is prohibitively high for solving large linear programs in $|A| \cdot |B| = O(n^2)$ variables with $|A| + |B| = O(n)$ constraints, with black-box solvers. ⁴
- Effect of noise in data on shape matching and registration is unknown, unreported or not analyzed

⁴[Mémoli, 2009], [Mémoli, 2011]

Contributions

- ▷ Establish a theoretical foundation for the use of Gromov-Hausdorff (GH) distance for point set registration with bi-Lipschitz deformation maps perturbed by Gaussian noise.
- ▷ Introduce a highly efficient iterative algorithm for point set matching with guaranteed convergence to a local minimum.
- ▷ Present a compressive stochastic registration framework, equipped with an efficient initialization scheme using multi-scale shape descriptors

The framework is adaptive to application and readily accepts prior information.

Chosen Deformation Family

By the desirable properties of (1) symmetric registration, (2) neighbor preservice and (3) insensitivity to noise, we model deformation f as surjective, Bi-Lipschitz

The **Bi-Lipschitz condition**:

$$\forall x \quad \exists r, r' > 0 \quad y \in N(x, r') \iff f(y) \in N(f(x), r) \quad (1)$$

This condition implies homeomorphism of f, f^{-1} .

Likelihood of Bi-Lipschitz Functions

Given observed data A, B , the likelihood distribution of Bi-Lipschitz functions is

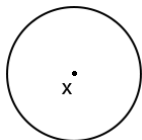
$$P(f | A, B) \triangleq P(f \text{ is bi-Lipschitz} | A, B)$$

To estimate the feasibility likelihood of f , we must consider

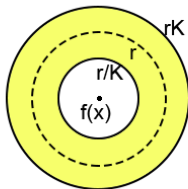
- the complexity for integrating over feasible locations
- the effect of noise on the feasibility criteria

Bi-Lipschitz condition

$$\forall x \quad \exists r, r' > 0 \quad y \in N(x, r') \iff f(y) \in N(f(x), r)$$



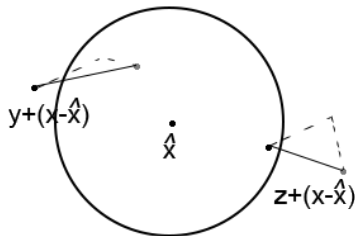
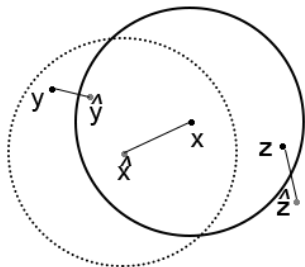
$N(x, r')$: Neighborhood of x with radius r'



$N(f(x), r)$: Neighborhood of $y = f(x)$ with radius r and deformation upper and lower bounds rK and r/K , respectively.

Under Gaussian Noise

Determine when points are *likely from* some neighborhood.



- (a) The neighborhood of x perturbed by noise. (b) A 2-point probabilistically equivalent noise model.

Log Likelihood by Aggregated Two-Point Feasibilities

$$P(f | A, B) \triangleq P(f \text{ is homeomorphic} | A, B) \propto \int_{(U, V) \in \delta_f^n} \mu(U) \mu(V) \\ \approx \prod_{a_j, a_l, f(a_j), f(a_l)} \int_{(u_1, u_2, v_1, v_2) \in \delta_f^2(a_j, a_l, f(a_j), f(a_l))} \mu(u_1, u_2) \mu(v_1, v_2)$$

$$\log P(f | A, B) \approx \sum_{a_j, a_l, f(a_j), f(a_l)} D(d(a_j, a_l), d(f(a_j), f(a_l)))$$

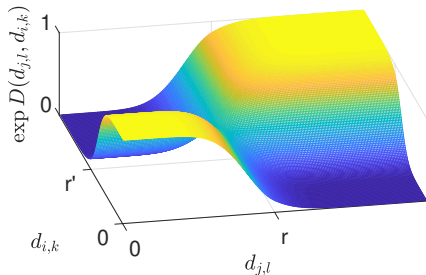
where

$$D(d(a_j, a_l), d(f(a_j), f(a_l))) \triangleq \log \int_{\delta_f^2} \mu(u_1, u_2) \mu(v_1, v_2)$$

Properties of Elementary 2-Point Likelihood

$D(d(a_j, a_l), d(f(a_j), f(a_l)))$ a function of point distance

by the radial neighborhood symmetry and the Bi-Lipschitz condition on f



Two-point likelihood (exponentiated) as a function of $d(a, a')$ and $d(b, b')$
(Lipschitz K not bounded)

L_2 GH Auxiliary Function

By the properties of 2-point likelihood $D(d(a, a'), d(b, b'))$

- ▶ It is largest when $d(a, a')$ and $d(b, b')$ are nearly equal.
- ▶ It is bounded by the bi-Lipschitz condition,

$$d(f(a), f(a')) \in \Theta(d(a, a'))$$

We substitute

$$\arg \max_f \sum_{j,l} D(d(a_j, a_l), d(b_j = f(a_j), b_l = f(a_l)))$$

by the $L_2 - GH$

$$\arg \min_f \sum_{j,l} \|d(a_j, a_l) - d(b_j = f(a_j), b_l = f(a_l))\|_2^2$$

Quadratic Program with Linear Constraints

$$\arg \min_{\Delta} \left\| \Delta d(A) \Delta^T - d(B) \right\|_F^2 - \sum_{i,j} \log P(f(a_j) = b_i) \Delta_{i,j}$$

Δ doubly stochastic.

for $\Delta_{i,j} = \delta(f(a_j) = b_i)$ and priors $P(f(a_j) = b_i)$.

- ▶ Integer program relaxation
- ▶ Non-convex
- ▶ Linearly constrained
- ▶ Quadratic in matching function (of size n^2)

Stochastic Matching Algorithm

Alternating optimization of Lagrangian following variable splitting

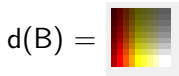
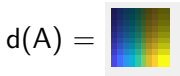
$$\arg \min_{y,x} y^T G y + \sum_{i,j} \log(P(f(a_j) = b_i)) \cdot y_{(i,j)} + \iota(x)$$

y is doubly stochastic.

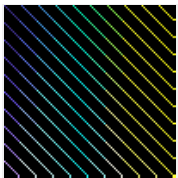
$y = x$ ties constraint and objective variables

$\iota(\cdot)$ is infinite where $P(f(a_j) = b_i) = 0$ and $x_{(i,j)} > 1$, $x_{(i,j)} < 0$.

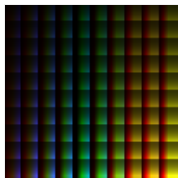
The Quadratic function



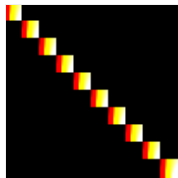
$$G = d(A)^2 \otimes I_n - 2 \cdot d(A) \otimes d(B) + I_n \otimes d(B)^2$$



sparse



dense



sparse

Convergence & Complexity

Guarantee convergence to local minimum. ⁵

Efficient use of problem structure:

1. Quadratic form of size $n^2 \times n^2$ admits special structure.
2. Solution to large system via block LU decomposition.
3. Supported by eigen-decomposition of distance matrices and LU of Schur complement.

Yields efficient computation:

1. Initialization requires $\mathcal{O}(n^3)$.
2. Each iteration requires $\mathcal{O}(n^3)$.

⁵[Wang et al., 2019]

Compressive Stochastic Registration Framework

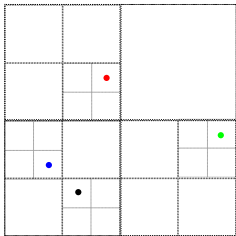
Initialization: $A_0 = A$, initial map f_0

1. Locate an auxiliary map f_k in compressive form,
 $f_k : A_k \subset \Omega_1 \rightarrow B \subset \Omega_2$
2. Remove outlier point pairings
3. Transform points, $A_{k+1} \leftarrow f_k(A_k)$

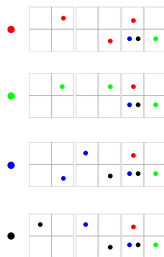
Obtain decompressed registration f from f_k .

Configuration Initialization: f_0

The configuration is initialized using Log-Cartesian feature, a multi-scale variant of Shape Context.⁶



(a) A 3-level grid used in creating the Log-Cartesian feature.



(b) Concatenated output grids which define histogram bins the Log-Cartesian feature.

⁶[Belongie et al., 2002]

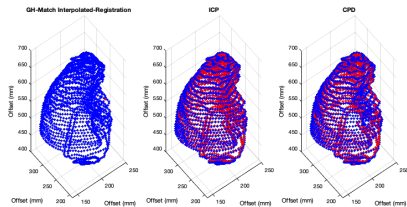
Data Description & Experiment Setup

- ▶ Respiratory motion data set of five patients at 14 amplitude binned respiratory phases ⁷ .
- ▶ Ground truth deformation is obtained by manual alignment of XCAT models to MRI data.
- ▶ For the experiments synthetic additive Gaussian displacements were added with variance set to a percentage of the true displacement magnitude.

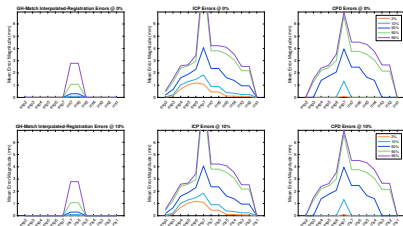
⁷[Konik et al., 2014]

Comparisons

- ▶ Our Compressive Stochastic Registration
- ▶ Iterative Closest Point ⁸
- ▶ Coherent Point Drift ⁹



(a) Registration results, source in registered red and target in blue for Patient M012.

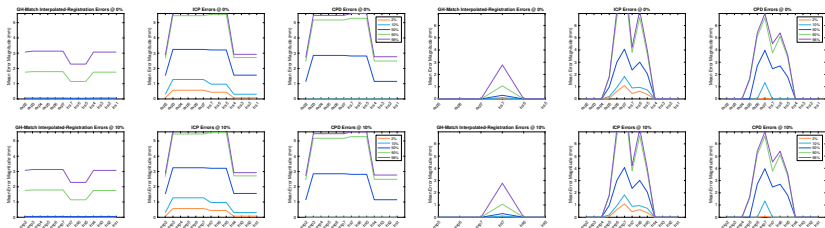


(b) Plots of error percentiles for Patient M012.

⁸[Besl and McKay, 1992]

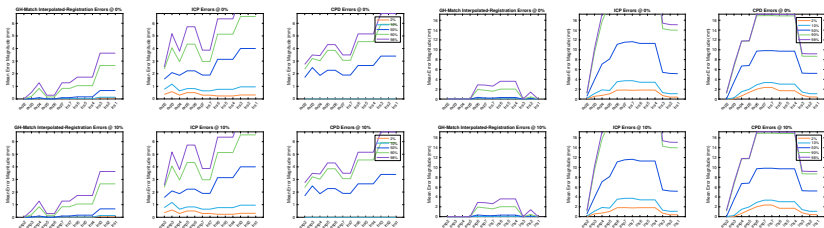
⁹[Myronenko and Song, 2010]

More Comparison Results



(a) Plots of error percentiles for Patient M001. (b) Plots of error percentiles for Patient M014.

More Comparison Results



(a) Plots of error percentiles for Patient M022. (b) Plots of error percentiles for Patient M023.

Recap

1. Analysis of noise in registration of functions under bi-Lipschitz transformations
2. Exploitive iterative algorithm with garaunteed convergence
3. Compressive Registration Framework
4. Efficient Log-Cartesian Shape feature

Questions?

References (1)



Belongie, S., Malik, J., and Puzicha, J. (2002).

Shape matching and object recognition using shape contexts.

IEEE Transactions on Pattern Analysis and Machine Intelligence,
24(4):509–522.



Besl, P. J. and McKay, N. D. (1992).

A method for registration of 3-D shapes.

IEEE Transactions on Pattern Analysis and Machine Intelligence,
14(2):239–256.



Chui, H. and Rangarajan, A. (2003).

A new point matching algorithm for non-rigid registration.

Computer Vision and Image Understanding, 89(2-3):114–141.
cited By 1045.

References (2)

 Heckemann, R. A., Hajnal, J. V., Aljabar, P., Rueckert, D., and Hammers, A. (2006).

Automatic anatomical brain mri segmentation combining label propagation and decision fusion.




NeuroImage, 33(1):115 – 126.

 Konik, A., Connolly, C. M., Johnson, K. L., Dasari, P., Segars, P. W., Pretorius, P. H., Lindsay, C., Dey, J., and King, M. A. (2014).




Digital anthropomorphic phantoms of non-rigid human respiratory and voluntary body motion for investigating motion correction in emission imaging.

Phys Med Biol, 59(14):3669–3682.




References (3)

-  Lempitsky, V. and Boykov, Y. (2007).
Global optimization for shape fitting.
In 2007 IEEE Conference on Computer Vision and Pattern Recognition,
pages 1–8.
-  Mémoli, F. (2009).
Spectral Gromov-Wasserstein distances for shape matching.
In 2009 IEEE 12th International Conference on Computer Vision Workshops, ICCV Workshops, pages 256–263.
-  Mémoli, F. (2011).
Gromov-Wasserstein distances and the metric approach to object matching.
Foundations of Computational Mathematics, 11(4):417–487.

References (4)

-  Myronenko, A. and Song, X. (2010).
Point set registration: Coherent point drift.
IEEE Transactions on Pattern Analysis and Machine Intelligence,
32(12):2262–2275.
-  Simon, A., Nassef, M., Rigaud, B., Cazoulat, G., Castelli, J., Lafond, C., Acosta, O., Haignon, P., and de Crevoisier, R. (2015).
Roles of Deformable Image Registration in adaptive RT: From contour propagation to dose monitoring.
Conf Proc IEEE Eng Med Biol Soc, 2015:5215–5218.
-  Sun, J., Ovsjanikov, M., and Guibas, L. (2009).
A concise and provably informative multi-scale signature based on heat diffusion.
In *Proceedings of the Symposium on Geometry Processing*, SGP '09, pages 1383–1392, Aire-la-Ville, Switzerland, Switzerland. Eurographics Association.

References (5)

-  Terwilliger, T. C., Sobolev, O. V., Afonine, P. V., and Adams, P. D. (2018). Automated map sharpening by maximization of detail and connectivity. *Acta Crystallographica Section D*, 74(6):545–559.
-  Thompson, D. W. (1992). *On Growth and Form*. Canto. Cambridge University Press.
-  Wang, Y., Yin, W., and Zeng, J. (2019). Global convergence of ADMM in nonconvex nonsmooth optimization. *Journal of Scientific Computing*, 78(1):29–63.